

Supplemental Information

Modeling the Kinetics of Lipid-Nanoparticle-Mediated Delivery of Multiple siRNAs to Evaluate the Effect on Competition for Ago2

Radu Mihaila, Dipali Ruhela, Beverly Galinski, Ananda Card, Mark Cancilla, Timothy Shadel, Jing Kang, Samnang Tep, Jie Wei, R. Matthew Haas, Jeremy Caldwell, W. Michael Flanagan, Nelly Kuklin, Elena Cherkaev, and Brandon Ason

Table 1. Description of the various model variables and model parameters used to optimize the model.

Model Variables	Description	Initial Value at t=0 (molecules)
x_1, y_1^*	Extracellular LNP	10 nM, 60 nM ¹
x_2, y_2	Endosomal LNP	0
x_3, y_3	Free Sirna (cytoplasm)	0
z	Ago2	6200 copies per cell ¹
x_4, y_4	Ago2 bound siRNA	0
x_5, y_5	Active RISC-mRNA	0
x_6, y_6	mRNA	100 copies per cell ²
E	Extracellular Compartment	3E-4 L ²
I	Intracellular Compartment	1.4E-12 L ²
Model Parameters	Description	Value
a	LNP crossing the plasma membrane	0.005 1/hr ²
b	endosomal escape/ unpackaging	5.00E-04 1/hr ²
c	lysosomal degradation	3 1/hr ²
d_i, d_{ii}	siRNA loading onto RISC	0.001 1/nM*hr ²
e	Degradation of siRNA in the cytoplasm	0.03 1/hr ²
f	formation of active RISC with target mRNA	0.1 1/nM*hr ²
g	cleavage of target mRNA by RISC	7.2 1/hr ²
h	transcription rate of mRNA	100 copies/hr ²
k	degradation of mRNA	1 1/hr ²
time of escape, b_{R_RNAiMAX}		5-20 min, 0.01 ²
time of escape, b_{L_LNP}		1.5-2 hours, 0.002 ²

*x denotes the target siRNA and y denotes the competitor siRNA, ¹Values determined experimentally, ²Values obtained from Ref 30

Table 2. siRNA sequences. The following chemical modifications were added to the 2' position of the ribose sugar when indicated: deoxy (d), 2' fluoro (f), or 2' O-methyl (o). Modification abbreviations are listed immediately preceding the base to which they were applied. Passenger sequences were capped with an inverted abasic nucleotide on the 5' and 3' ends (iB).

siRNA	guide sequence	passenger sequence
Ago2(722)	rA;rC;rU;fluU;fluC;omeA;fluC;omeA;omeA;omeA;fluC;omeA;omeA;rA;fluC;fluU;fluC;omeG;omeA;omeU;omeU	iB;fluU;fluC;dG;dA;dG;fluU;fluU;fluU;dG;fluU;dG;dA;dG;fluU;dT;dT;B
Apoa4(548)	rG;rU;rA;fluC;omeG;omeA;fluC;omeA;omeA;omeA;omeG;omeG;omeG;omeA;fluC;omeA;omeG;omeU;omeU	iB;fluC;fluU;dG;dG;fluU;dG;fluC;fluC;fluU;fluU;dG;fluU;fluC;dG;fluU;dA;fluC;dT;dT;B
Apoa4(810)	rU;rC;rC;omeA;fluC;omeA;fluU;fluU;fluC;fluC;fluU;omeG;omeA;fluU;fluC;omeG;omeU	iB;fluC;dG;dA;fluU;fluC;dA;dA;dG;dG;dA;dG;dA;fluU;dG;fluU;dG;dA;dT;dT;B
ApoB(19)	rU;rU;rU;fluC;omeA;omeA;fluU;omeG;fluU;omeA;fluU;omeG;fluU;omeG;omeA;omeG;omeU;omeU	iB;fluC;fluU;fluC;fluU;fluC;dA;fluC;dA;fluU;dA;fluC;dA;fluU;fluU;dG;dA;dA;dT;dT;B
Control siRNA	fluC;fluC;fluU;omeG;omeA;omeA;omeG;omeA;omeG;omeA;omeG;fluU;fluU;omeA;omeA;omeA;rA;rG;rA;omeU;omeU	iB;fluU;fluC;fluU;fluU;fluU;dA;fluC;fluU;fluC;fluU;fluU;fluU;fluU;dA;dG;dG;dT;dT;B
Serpina6(1011)	rU;rG;rC;omeG;omeA;omeA;omeA;fluU;fluC;omeA;omeG;omeA;fluU;omeG;omeG;fluU;omeG;omeU;omeU	iB;fluC;dA;dA;fluC;fluC;dA;dA;fluU;fluU;dG;dA;fluU;fluU;fluU;fluC;dG;fluC;dA;dT;dT;B
SSB(291)	rU;rU;rA;fluC;omeA;fluU;fluU;omeA;omeA;omeA;omeG;fluU;fluC;fluU;omeG;fluU;fluU;omeG;fluU;omeU;omeU	iB;dA;fluC;dA;dA;fluC;dA;dG;dA;fluC;fluU;fluU;fluU;dA;dA;fluU;dG;fluU;dA;dA;dT;dT;B

Fig. 1. Results of numerical simulated kinetics of ApoB(19) + competitor siRNA SSB(291) using RNAiMax and LNP. Simulation kinetics of mRNA knockdown of target siRNA ApoB(19) (red solid line) with competitor SSB (291) (blue line) upon delivery by RNAiMax (A) and LNP (B). Simulation kinetics of Ago2 loading of target siRNA ApoB(19) (red dotted line) with competitor SSB (291) (blue dotted line) upon delivery by RNAiMax (C) and LNP (D). Ago2 levels are shown in purple.

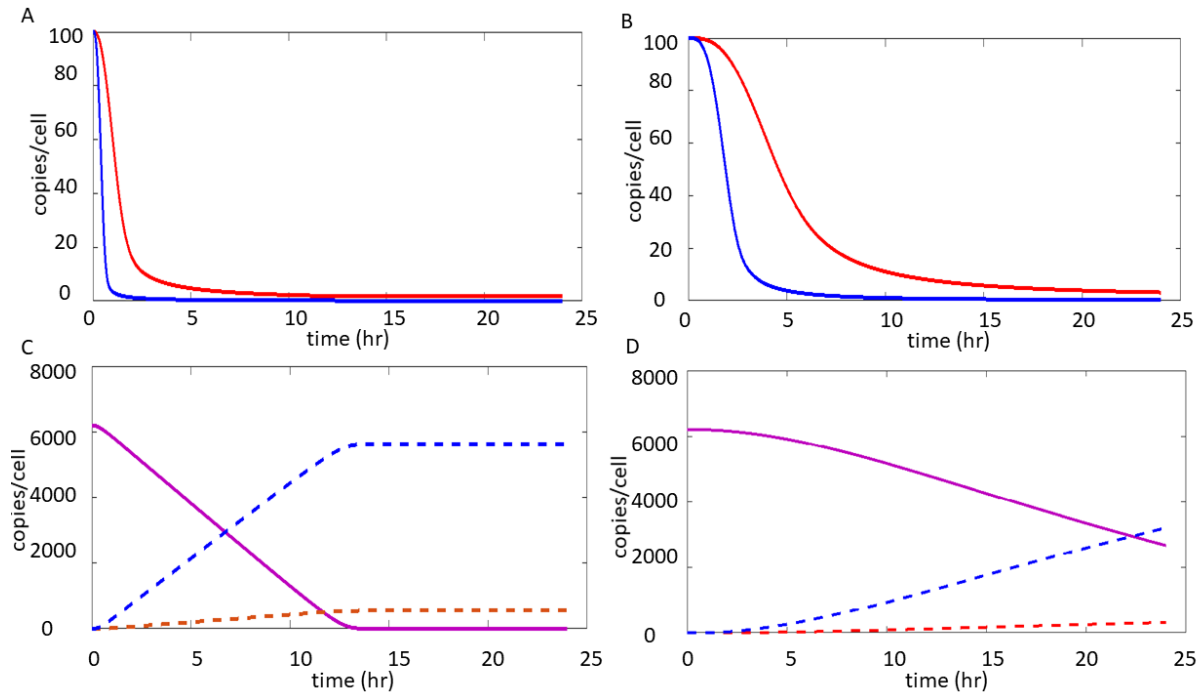


Fig. 2. Kinetics of ApoA4(548) binding to Ago2 using LNP or RNAiMax mediated delivery. A greater amount of ApoA4(548) siRNA bound by Ago2 was observed for RNAiMax mediated delivery relative to LNP at 0.5 and 1.5 hrs post-treatment. Data represented as the difference in signal (dCt) for ApoA4 relative to miR-16, which served as an internal control (bars +/- S.D., n= 3 biological replicates / condition). Significance calculated using a one-way ANOVA, Tukey post-test (***) = $p < 0.0001$).

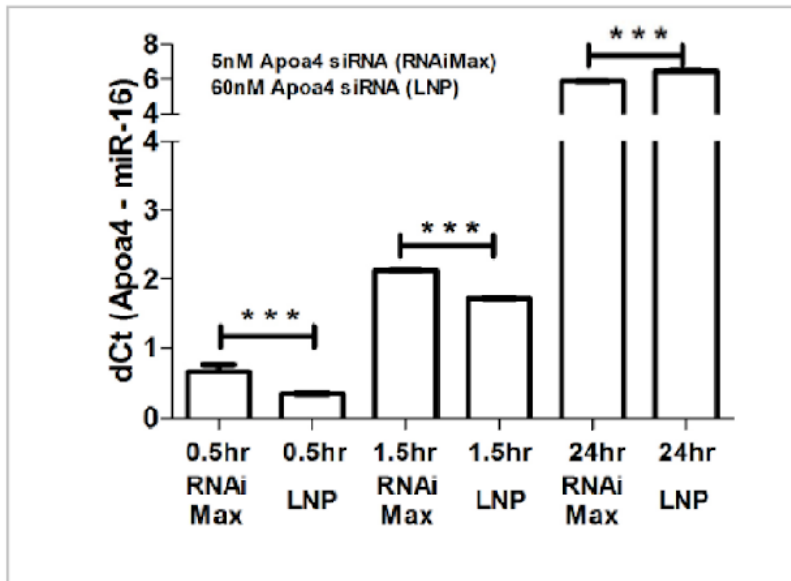


Fig. 3. A representative 52,000× Cryo-EM image of the low-PEG/high-cholesterol nanoparticle formulation (60% cationic lipid, 38% cholesterol and 2% PEG) in this study. The figure reveals a diversity of LNP sizes, shapes and lamellar properties within a single population. For example, most low-PEG/high-cholesterol particles in this image demonstrate a uniform distribution of multilamellar substructure whereas others have internal void spaces and/or elongated protrusions extending from their outer surface.

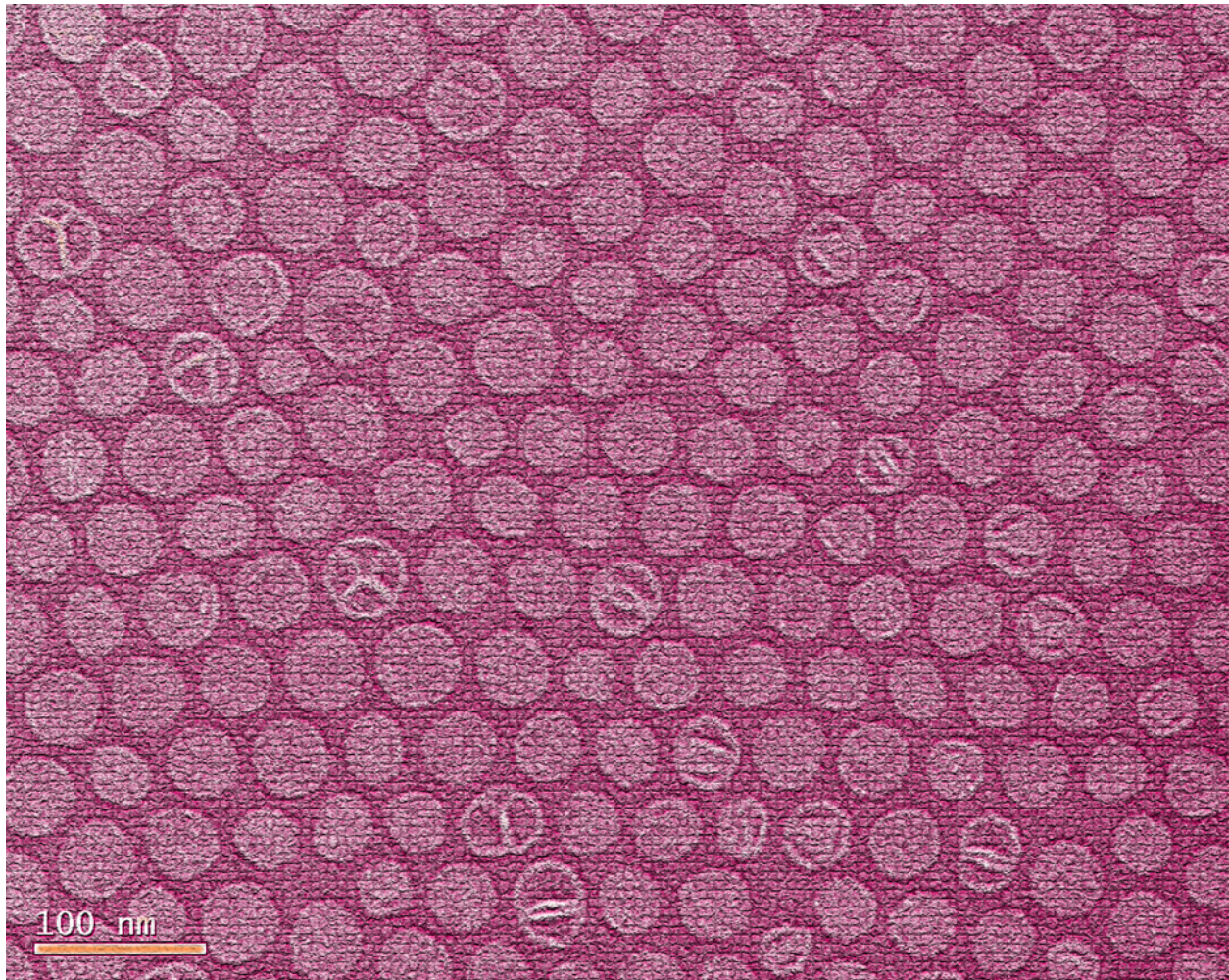


Fig. 4. Thermal analysis using VP DSC - siRNA-RNAiMax lipoplexes and LNP were analyzed by microcalorimetry using VP DSC (Microcal) under transfection conditions. Equal volumes (0.5 ml) of siRNA duplexes, RNAiMax, and LNP were suspended in an Opti-MEM solution and injected into the sample cells. The reference cells were filled with the Opti-MEM solution. The samples were thermally equilibrated to 5 °C and scanned from 5 °C to 110 °C at a scanning rate of 60 °C/hour. The heat capacity difference between the sample cell and the reference cell was plotted as a function of temperature.

